Available online at www.sciencedirect.com
ScienceDirect
Fuzzy Sets and Systems 158 (2007) 215–229
FUZZY sets and systems
www.elsevier.com/locate/fss

# Region-based fit of color homogeneity measures for fuzzy image segmentation☆

B. Prados-Suárez[a,*], J. Chamorro-Martínez[b], D. Sánchez[b], J. Abad[b]

[a]*Department of Computer Science, University of Jaén, C/ Alfonso X El Sabio 28, 23700, Linares, Jaen, Spain*
[b]*Department of Computer Science and Artificial Intelligence, University of Granada, C/ Periodista Daniel Saucedo Aranda s/n, 18071 Granada, Spain*

Available online 20 October 2006

**Abstract**

In this paper we introduce an approach to automatically select a homogeneity measure for color image segmentation, on the basis of the characteristics of the region to be segmented. In a previous work we presented a fuzzy color path-based image segmentation proposal where membership degrees were computed from the connectivity between pixels, based on the homogeneity degree of the path joining them. To measure homogeneity, we aggregate resemblances between consecutive pixels using t-norms. Since a great variety of homogeneity measures can be found, we need to automatically select a suitable t-norm for a given region. For this purpose we firstly approximate a value characterizing the region surrounding the seed, studying a set of fixed paths. Secondly, we establish a functional relationship between this value and the parameter of a Weber t-norm. Based on this functional relationship we obtain the value of t-norm's parameter, corresponding to the homogeneity measure to be used in the segmentation process. We show that our approach performs well in different types of regions.


*Keywords:* Image segmentation; Fuzzy segmentation; Path-based segmentation; Fuzzy connectivity; Fuzzy color homogeneity

## 1. Introduction

Image segmentation is the process of partitioning the image into connected subsets of pixels, called regions, on the basis of some homogeneity criteria. It is used in many image analysis techniques and applications, like image database retrieval, medical imaging or robot vision [2,12,27].

There are many segmentation techniques that provide a crisp segmentation of images, where each pixel belongs to a unique region [5,9,10,14,15,22,26]. However, this is not always a good solution since it cannot model imprecise regions, usually found in natural images, as occurs in shadows, brights and color gradients. This is why fuzzy segmentation techniques arise, defining a *region* as a fuzzy subset of pixels, where every pixel in the image has a membership degree to each region [1,3,8,11,18–20,23]. However, not all of these techniques take into account that a region must be topologically connected.

☆ This work has been supported by the MCYT (Spain) under Grant TIC2003-01504.
* Corresponding author.
*E-mail addresses:* belenps@ujaen.es (B. Prados-Suárez), jesus@decsai.ugr.es (J. Chamorro-Martínez), daniel@decsai.ugr.es (D. Sánchez), abad@decsai.ugr.es (J. Abad).

0165-0114/$ - see front matter © 2006 Elsevier B.V. All rights reserved.
doi:10.1016/j.fss.2006.10.006

To face up this problem, path-based techniques are employed, incorporating spatial information related to adjacency between pixels. Based on the idea of fuzzy topology, introduced by Rosenfeld [24], and the use of fuzzy connectivity to measure the relationship between any pair of pixels, these techniques obtain the fuzzy region by calculating the connectivity with respect to the seed of a region [1,7,13,17,21,25].

In [4] we proposed to calculate fuzzy connectivity of two pixels on the basis of what we called *homogeneity* of the "paths" connecting them. We calculate homogeneity as an aggregation of distances in color between consecutive pixels [1,6,16,21].

However, not every aggregation procedure is suitable for all the types of regions that can be found in an image. In real images there is a great variety of regions, with different homogeneity and contour characteristics, and for each kind of region a different aggregation operator should be used: the fuzzier the region and its contour is, the softer the aggregation should be. To determine the "best" operator for each region is a very important task, since otherwise the membership functions obtained do not represent adequately the fuzzy regions in the image. Our objective in this paper is to provide a way to select an aggregation operator suitable to model a fuzzy region.

As we saw in [4], the semantics of *homogeneity* suggest to employ t-norms as aggregation operators. Hence, our problem is to find the best t-norm for a given region. For that purpose, we employ Weber's parametric t-norm, and we try to establish a relationship between the $\lambda$ parameter and region characteristics.

The paper is organized as follows: in Section 2, after summarizing a methodology for path-based image segmentation, we propose an approach to automatically select a t-norm to be used in the segmentation process. This automatization is based in the computation of a value representing the region seed's environment characteristics, as shown in Section 3. In Section 4, we establish a functional relationship between this value and the $\lambda$ parameter of a Weber t-norm. In Sections 5 and 6 we show the results obtained applying this automatization and our conclusions.

## 2. Path based segmentation

In this section we summarize the path-based approach presented in [4] that incorporates spatial information about pixel adjacency by measuring the connectivity between any pair of pixels, as the homogeneity of the most homogeneous path joining them. Based on it, fuzzy image segmentation is performed computing the connectivity between each seed point and all the pixels in the image.

### 2.1. Pixel characterization

Firstly, to characterize a pixel, $p$, in the image, we use a feature vector, $\overrightarrow{f_p}$, where each feature, $f_p^i$, is a numerical measure of any relevant characteristic obtained for $p$. In our case, we are interested in obtaining homogeneously colored regions, so we have chosen the human perception based color space HSI (hue, saturation or purity and intensity or lightness) [4]. Hence, the feature vector we use to characterize each pixel $p$ in the image contains its three band color representation in the HSI color space, as shown below:

$$\overrightarrow{f_p} = [H_p, S_p, I_p]. \tag{1}$$

### 2.2. Fuzzy resemblance between neighbor pixels

Once we have characterized each pixel, a resemblance relation, denoted by $\mathcal{FR}$, between neighbor pixels is defined on the basis of the above mentioned feature vectors. The resemblance measure between features vectors depends on the specific features employed. In our case, feature vector resemblance is based on color resemblance, based on a distance defined in the HSI color space, $\Delta C(c_1, c_2)$. This distance is defined in [4] on the basis of the differences between color components, $\Delta_H$, $\Delta_S$ and $\Delta_I$ for hue, saturation and intensity values, respectively.

We define the resemblance between the feature vectors $f_p$ and $f_q$ corresponding to pixels $p$ and $q$ in the image $IM$ as shown below:

$$\mathcal{FR}(\overrightarrow{f_p}, \overrightarrow{f_q}) = 1 - \Delta C(\overrightarrow{f_p}, \overrightarrow{f_q}). \tag{2}$$

Finally, we define a resemblance relation $\mathcal{PR}$ between neighbor pixels, as the relation $\mathcal{FR}$ between their corresponding feature vectors:

$$\mathcal{PR}(p, q) = \mathcal{FR}(\overrightarrow{f_p}, \overrightarrow{f_q}). \tag{3}$$

### 2.3. Fuzzy connectivity between pixels

Though resemblance between feature vectors can be calculated for any pair of pixels, we restrict it to neighbor pixels because in image segmentation, topological information about the relative position of pixels is crucial. In order to group together pixels that belong to the same homogeneous region, we need to extend this relation to any pair of pixels of the image. This is called fuzzy connectivity. Fuzzy connectivity of two pixels indicates, in fuzzy path-based image segmentation, the degree to which those pixels belong to a group of topologically connected pixels with resemblant features.

The topological connection between pixels can be expressed by the notion of path. Given two pixels, $p$ and $q$, we defined in [4] the path joining them, $\pi_{pq}$, as the sequence

$$\pi_{pq} = (r_1, r_2, \ldots, r_k), \tag{4}$$

where $k \geqslant 1$, such that $r_1 = p$ and $r_k = q$ and $r_i$ is connected to $r_{i+1}$ $\forall i \in \{1, \ldots, k-1\}$. With $\Pi_{pq}$ we denote the set of all the possible paths between $p$ and $q$.

We say that two pixels are connected when there is a path linking them such that all the consecutive pixels in the path are resemblant. If this happens, we say that the path is *homogeneous* with respect to color. With this idea in mind, we defined the homogeneity of each path joining $p$ and $q$ as a measure $homo : \Pi_{pq} \to [0, 1]$, calculated on the basis of resemblance between consecutive points in the path as we shall see in the next subsection. Then, taking the *homo* function into account, we defined the optimum path between $p$ and $q$, $\hat{\pi}_{pq}$, as the path linking them with maximum homogeneity. Finally, on this basis, we get the measure of the connectivity between two pixels as the homogeneity value of the optimum path joining them, i.e.,

$$conn(p, q) = homo(\hat{\pi}_{pq}). \tag{5}$$

As a final remark, the aforementioned fuzzy connectivity between two pixels lets us define below the membership degree of a pixel $p$, to a region $\widetilde{R_s}$, as the connectivity between the pixel and the seed point, $r_s$, of the region:

$$\mu_{\widetilde{R_s}}(p) = conn(p, r_s). \tag{6}$$

Computing the membership degree of each point $p$ in the image to each region $\widetilde{R_s}$, we obtain the set of fuzzy regions resulting of the fuzzy segmentation process, with a computational cost of $O(uv)$, as detailed in [2], with $u$ being the size of the image and $v$ being the number of seeds.

### 2.4. Homogeneity measures

In [4] we studied the characteristics that homogeneity measures should verify, and we concluded that a natural way to define them is to perform an aggregation of resemblances between pairs of consecutive points in the path by means of a t-norm. Using a t-norm is coherent with the idea that *all* the pairs of consecutive pixels must be resemblant for the path to be homogeneous.

The immediate question is, what t-norm to use? In [4] we studied bounded difference, algebraic product and also t-norms of Frank, Dubois and Prade and Weber. In the last three cases we have parametric functions that show different behaviors depending on the value of their parameter. In particular, Weber's parametric t-norm

$$W(a, b, \lambda) = \max\left\{0, \frac{a + b + ab\lambda - 1}{1 + \lambda}\right\}, \tag{7}$$

where $\lambda > -1$, covers a wide range of behaviors. As the values of $\lambda$ change from $-1$ to 0 and above, the resulting t-norm becomes less strict. Because of that, in [4] we decided to employ this t-norm in our work.

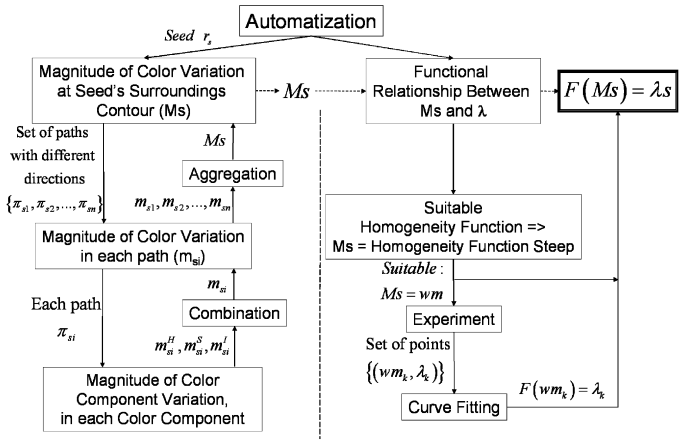


Fig. 1. Scheme of the automatic selection procedure of $\lambda$ parameter for a given region seed.

Our main conclusion is that no t-norm is better than the rest in all the situations. In real images we can find several types of regions according to their homogeneity and contour characteristics. Regions vary between two extreme situations: on the one hand, homogeneous regions with well defined contours; on the other hand, there are regions with very soft changes from the color inside the region to the one outside, the most representative case being a soft tone down. Between these extreme situations, there are a great variety of regions, where contours become wider and softer.

We consider that the type of region determines the t-norm we should employ. In the case of a region with a well defined contour, the best option is to use a more strict t-norm that yield low values as it finds large difference values in color, something that happens in the contour. This way, the difference between the support and the kernel of the membership function of the fuzzy region will be smaller, as the region is more crisp. An example on these functions is Weber t-norm with $\lambda$ around $-0.8$. On the other hand, if region is a soft tone down we should choose a less strict t-norm, like Weber t-norm with $\lambda$ around 0. Intermediate cases are fit by intermediate $\lambda$ values.

The next natural step is, given a seed, to select a $\lambda$ value such that the behavior of the corresponding t-norm fits the homogeneity characteristics of the region around that seed. This is the topic we face in Section 2.5.

### *2.5. Automatic selection of Weber t-norms*

As we pointed out in the previous section, the difference between types of regions lies on the characteristics of their contours (from narrow and abrupt to wide and soft). Hence, it seems natural to choose the value $\lambda$ of the Weber t-norm on the basis of an analysis of the contour of the region.

Therefore, in order to automatically select a Weber t-norm (a $\lambda$ value) for a given seed we propose an approach consisting of two steps (Fig. 1). First, we will characterize by means of a real value the magnitude of color variation in the contour of the region for a given seed; second, we shall employ this value to determine the parameter $\lambda$. For that purpose, we shall establish a functional relationship between them. These two steps will be explained in detail in Sections 3 and 4, respectively.

## 3. Measuring color variation in region contours

The problem posed in this section is, given a seed point, to obtain a value representing the color change in its contours. To face it, a first approach could be to study the evolution of the color values around the seed, viewing them as a bidimensional surface. Since we work with paths, here we propose to use a different approach that consists in studying a set of paths covering the main directions around the seed, and to compute the magnitude of color change in each of them.

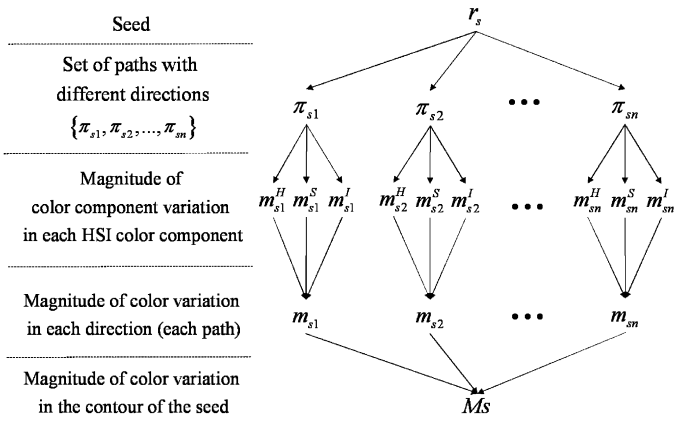


Fig. 2. Scheme summarizing the steps followed to obtain a value, $M_s$, representing the magnitude of color change in the contour of the area around the seed.

In this paper, the paths we have chosen are straight lines homogeneously distributed through different directions around the seed, with a length according to the target region's size. We shall denote each path in the set as $\pi_{si}$, where $s$ represents the seed pixel, $i$ is the index of a path in the set $\{\pi_{s1}, \pi_{s2}, \ldots, \pi_{sn}\}$, and $n$ is the number of paths in the set.

Once we have chosen the set of paths, we study each of them, looking for significant color variations. In Section 3.1 we obtain a value characterizing the magnitude of color variation in a single path. After this procedure has been applied to all the paths, we obtain a set of values. These values are aggregated in order to summarize the information coming from all of them as explained in Section 3.2. The result is the value representative of the color variation for the region corresponding to the given seed. Fig. 2 shows a scheme of the whole process.

### *3.1. Measuring color variation in each path*

In order to measure the color variation in each path, we first study the variation in each color component (Section 3.1.1), and then we combine the information obtained in each channel (Section 3.1.2).

#### *3.1.1. Color component analysis*

In this section, given a path $\pi_{si}$, we study the information in each color component separately. We shall analyze each component in the same way, so we shall describe the analysis for a generic component $\Phi \in \{H, S, I\}$.

Our analysis will be based on the concept of profile of a component $\Phi$ along a path, defined as follows:

**Definition 3.1.** We define the profile of a color component $\Phi$ along a path $\pi_{si}$ as the function giving, for each point along the path, its value on that color component, i.e.,

$$P^{\Phi}_{\pi_{si}}(r) = \Phi_r, \tag{8}$$

where $r \in \pi_{si}$ and $\Phi_r$ represents the value of the component $\Phi$ at the point $r$. For the hue component we have to take into account the circularity property. Let us also remark that when we calculate the profiles, for those colors corresponding to achromatic areas, we modify the $H$ and $S$ value to be a new value "undefined", and in the case of semichromatic areas we do the same only with $H$, so that the final profile corresponding to a low saturated or low intensity area is plain for the components involved.

As an example, images (B2,C2,D2) of Fig. 5 shows the hue, saturation and intensity profiles, respectively, as a red continuous line, for the horizontal path marked as a red line in Fig. 5(E). Intuitively, these profiles represent the behavior of the region in the direction followed by the path.

The most important part of the profile for us is that corresponding to the contour of the region. If the area around the seed is homogeneous with a well defined contour, the values of the profile will be very similar up to a point

where there will be a big change in the values. On the contrary, if the region is a tone down, the profile values will be decreasing/increasing at a constant rate.

In a certain profile, contours are delimited by relevant variations in the values. In order to detect such variations, we shall study the gradient of the profile, i.e., differences between values at consecutive points. Specifically, the local extremes of the gradient indicate the presence of contours. This leads us to the following definition:

**Definition 3.2.** We define a relevant color component variation point in the profile $P^{\Phi}_{\pi_{si}}$, denoted by $v^{\Phi}_{si}$, as the local extreme point (maximum or minimum) in the path whose gradient magnitude is over a given relevance threshold, $T^{\Phi}_{si}$.

In this paper, we compute the relevance threshold, $T^{\Phi}_{si}$, as a given percentage of the magnitude of the highest peak of the gradient, in absolute value.

Given a path $\pi_{si}$ there will be a set of relevant color component variation points. We shall choose one of them, denoted by $\hat{v}^{\Phi}_{si}$, as an indicator of the first contour. In this paper, for the case of the HSI color space, we propose to firstly compute $\hat{v}^{H}_{si}$ as the first relevant variation point in the path, and then search for $\hat{v}^{S}_{si}$ and $\hat{v}^{I}_{si}$ in a fixed interval around $\hat{v}^{H}_{si}$. If no relevant variation point is found in the hue component, we start the analysis in saturation and if again there is no such points in the saturation profile, we look for them in the intensity profile. This ordering, together with the way we obtain the profiles, allows us to overcome the problem of undefined saturation and hue at low chromaticity conditions or gray scale images.

Once we have obtained $\hat{v}^{\Phi}_{si}$ for each component we approximate the magnitude of variation around those positions as

$$m^{\Phi}_{si} = \frac{P^{\Phi}_{\pi_{si}}(r\hat{v}^{\Phi}_{si}) - P^{\Phi}_{\pi_{si}}(l\hat{v}^{\Phi}_{si})}{r\hat{v}^{\Phi}_{si} - l\hat{v}^{\Phi}_{si}}, \tag{9}$$

where $l\hat{v}^{\Phi}_{si}$ and $r\hat{v}^{\Phi}_{si}$ are the zero crosses in the gradient, on the left and right of $\hat{v}^{\Phi}_{si}$, respectively. They represent the points where the variation indicated by $\hat{v}^{\Phi}_{si}$ starts and ends, while $m^{\Phi}_{si}$ is the slope of the line that links them.

Fig. 5(B2,C2,D2) shows the gradient of the profile in each component as a green dotted curve, the position of the maximum local extreme in the profile gradient as a black triangle, the point $\hat{v}^{\Phi}_{si}$ marked as a red square, and the points $l\hat{v}^{\Phi}_{si}$ and $r\hat{v}^{\Phi}_{si}$ as blue circles.

### *3.1.2. Combination of color components information*

Given the three relevant color component variation points $\hat{v}^{H}_{si}$, $\hat{v}^{S}_{si}$ and $\hat{v}^{I}_{si}$, we combine their corresponding magnitudes $m^{H}_{si}$, $m^{S}_{si}$ and $m^{I}_{si}$ as

$$m_{si} = \sqrt{\frac{\left(m^{H}_{si}\right)^2 + \left(m^{S}_{si}\right)^2 + \left(m^{I}_{si}\right)^2}{3}}. \tag{10}$$

Since we are in a three-dimensional color space, the magnitudes $m^{H}_{si}$, $m^{S}_{si}$ and $m^{I}_{si}$ can be viewed as the module of the projection on each axis of the a vector giving the whole color variation. Under this point of view, the color variation at a contour point in the path, $m_{si}$, would be the module of this vector, as shown in Eq. (10).

## *3.2. Aggregation of path information*

In this paper, in order to avoid extreme cases, we have decided to choose the median in order to aggregate the values $m_{si}$ for each path, since it is an aggregation selecting an intermediate value. Therefore, the variation in the contour of the region associated to seed $r_s$, we denote by $M_s$, is

$$M_s = Median\{m_{si}\}, \tag{11}$$

where $i \in \{1..n\}$, $n$ is the number of paths employed in the analysis.

## 4. Functional relationship between $M_s$ and $\lambda$

In the previous section we characterized region contours by means of a slope measure $M$. Since we want to estimate the value $\lambda$ that fits a given contour, our objective is to find a function $\mathcal{F}$ relating $M$ and $\lambda$:

$$\begin{aligned} &\mathcal{F} : [0, 1] \to (-1, \infty), \\ &\quad \mathcal{F}(M) = \lambda. \end{aligned} \tag{12}$$

For that purpose, we shall perform an experiment in order to obtain a set of valid pairs of values (points) $\Psi = \{(M^1, \lambda^1), \ldots, (M^m, \lambda^m)\}$ and later we shall estimate $\mathcal{F}$ by fitting a suitable curve to the set of points $\Psi$.

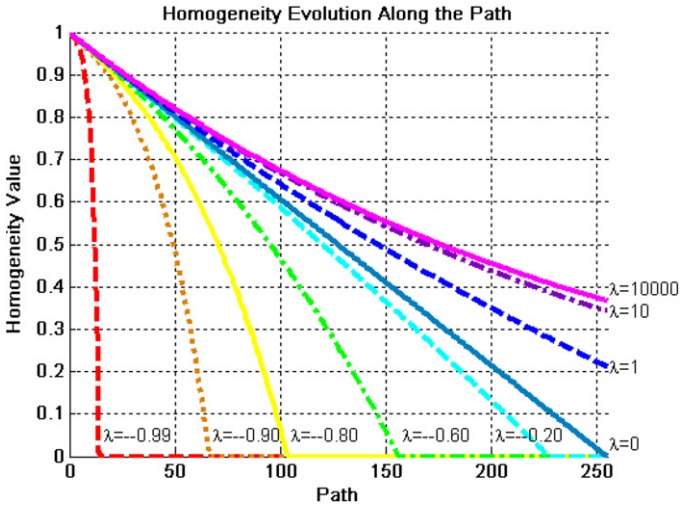


Fig. 3. Evolution of the homogeneity along a constant variation path using Weber's t-norm with different $\lambda$ values.

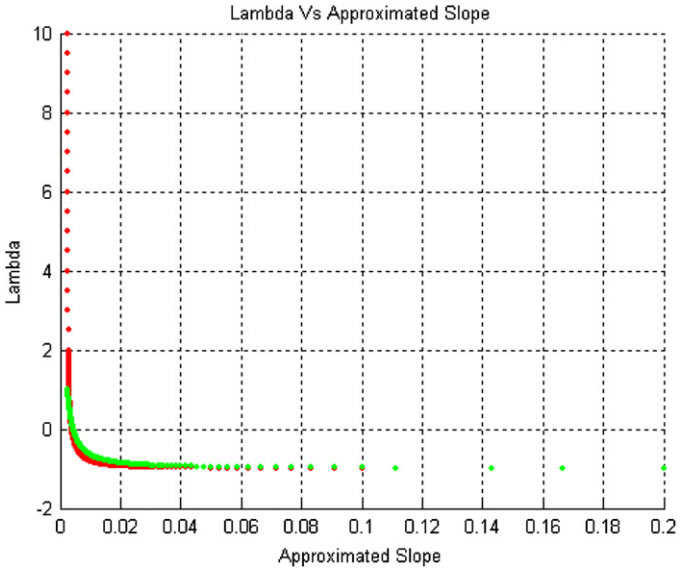


Fig. 4. Graphic representation of obtained points $(M^i, \lambda^i)$, in red. In green approximated function, $\mathcal{F}(M^i)$.

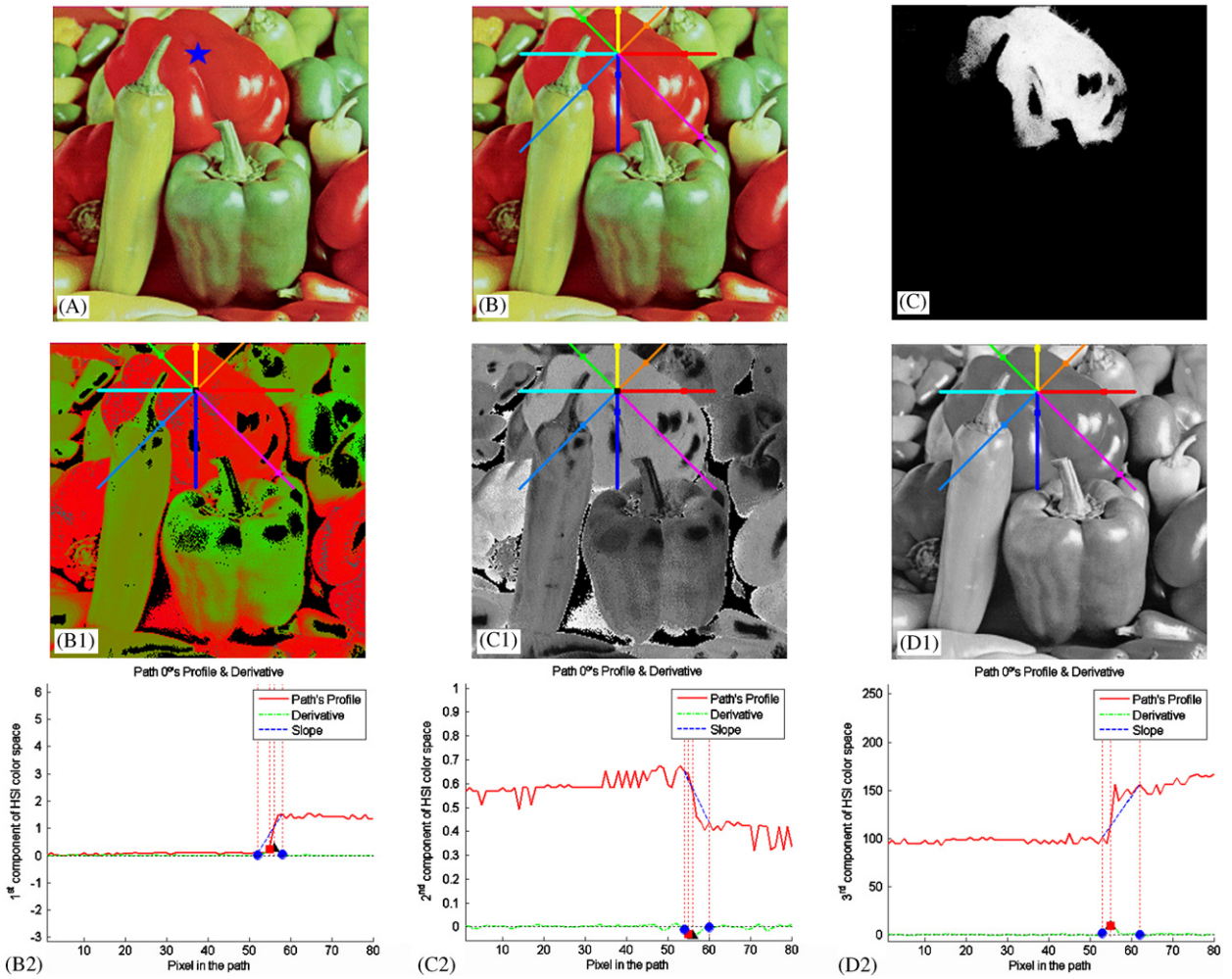


Fig. 5. Results obtained for a crisp region with the proposed approach. A: the original image with the seed in the star. B1,C1,D1: the hue, saturation and intensity images, respectively, with paths used and the detected $\hat{v}$ points. B2,C2,D2: hue, saturation and intensity profiles for the 0° path, respectively. E: original image with the final first relevant color variation points detected in each direction. F: the final fuzzy region.

### 4.1. *Finding a set $\Psi$ of pairs $(M, \lambda)$*

We propose the following set of properties to be verified by $\Psi$:

(1) The value $\lambda = 0$ will be associated to a path of constant variation $K$ (that implies $M = K$).
(2) For a given pair $(M^i, \lambda^i)$, $M^i > K$ implies $\lambda^i < 0$. In the same way, $M^i < K$ implies $\lambda^i > 0$.
(3) If $M^i > M^j$ then $\lambda^i < \lambda^j$. In the same way, if $M^i < M^j$ then $\lambda^i > \lambda^j$.

In this paper we have fixed $K = \frac{1}{255}$, corresponding to the minimum possible normalized variation in the intensity component. This value corresponds to a (not normalized) variation of $1'22°$ in the hue component, or a variation of 0.0068 in the saturation component.

Taking into account the previous properties, we suggest to obtain $\Psi$ as follows: given a theoretical path where the resemblance between consecutive pixels is constant and equal to $K$, we represent the evolution of the homogeneity along the path, for a specific $\lambda$, as a function. For each pixel $p$ in the path, the value of this function corresponds to the homogeneity of the subpath that goes from the first pixel to $p$. Obviously, this is a decreasing function that goes from $(0, 1)$ to $(x_\lambda, 0)$. Fig. 3 shows this homogeneity evolution function for several values of $\lambda$.

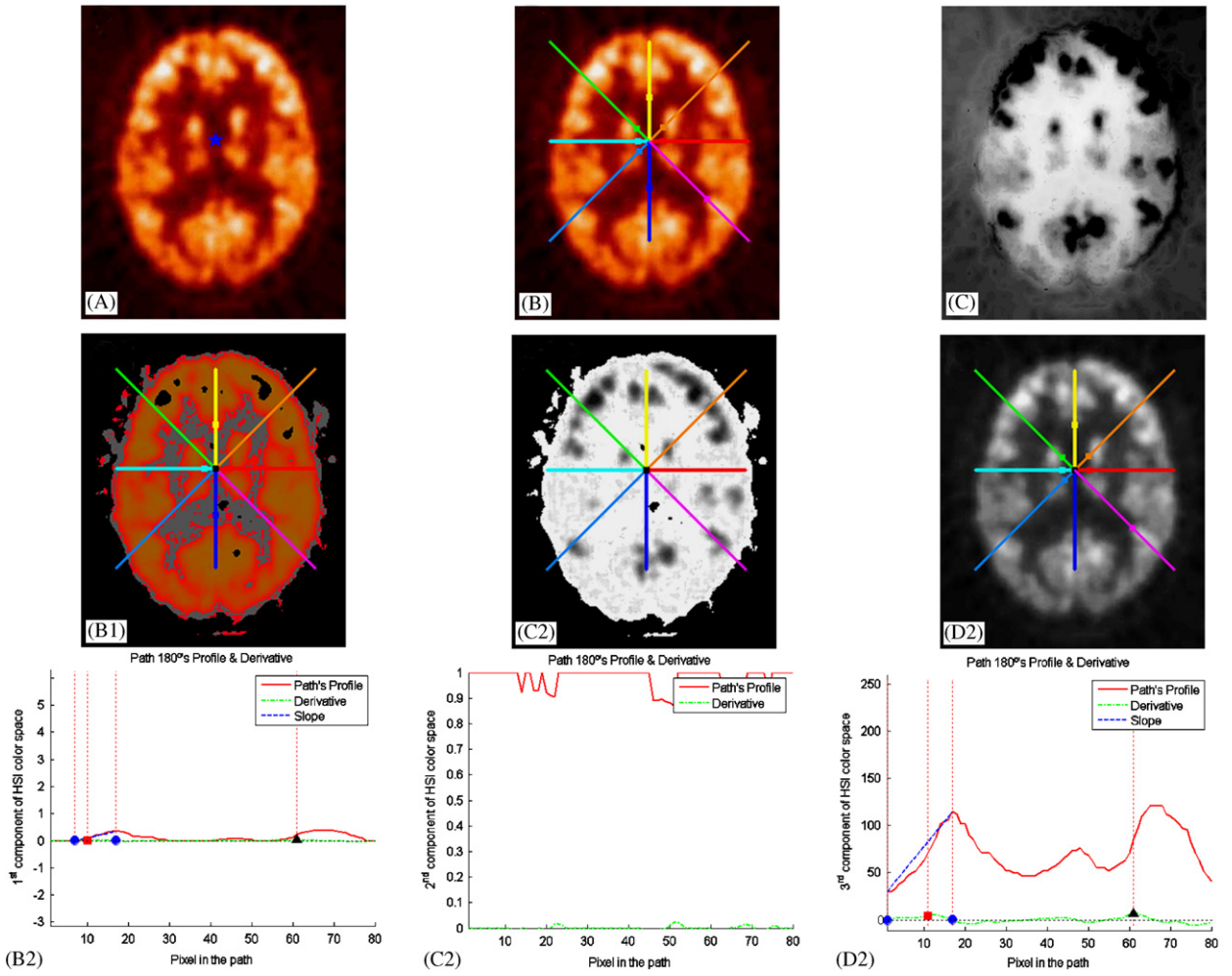


Fig. 6. Results obtained on an imprecise contour region with the proposed approach. A: the original image with the seed in the star. B1,C1,D1: the hue, saturation and intensity images, respectively, with paths used and the detected $\hat{v}$ points. B2,C2,D2: hue, saturation and intensity profiles for the 180° path, respectively. E: original image with the final first relevant color variation points detected in each direction. F: the final fuzzy region.

From these functions we obtain $\Psi$. Given a fixed set of $\lambda$ values $\lambda^1, \ldots, \lambda^m$, the corresponding slope values $M^1, \ldots, M^m$ are obtained as follows: given a $\lambda^i$, the corresponding $M^i$ is the slope of the line between the points $(0, 1)$ and $(x_{\lambda^i}, 0)$. Let us remark that, as can be seen in Fig. 3, for $\lambda = 0$, this line matches exactly a line with slope $K = \frac{1}{255}$, hence $M^i = K = \frac{1}{255}$.

Fig. 4 shows the set $\Psi$ we have obtained, marked with red points, with $m = 3000$.

### 4.2. *Fitting a function $\mathcal{F}$ to $\Psi$*

By looking at the red line in Fig. 4 it can be easily appreciated that this graphic representation has two asymptotes, one horizontal in $\lambda = -1$, because it is the minimum value of $\lambda$, and another one vertical in $M = 0$, the minimum possible slope, corresponding to a homogeneous region. In addition, it may be appreciated that the real interval in which the slope varies is approximately $(0, 0.2]$. We concluded that function $\mathcal{F}(M)$ may be approximated by a rational function on the absolute value of the slope, and displaced one unit down because of the vertical asymptote. In addition,

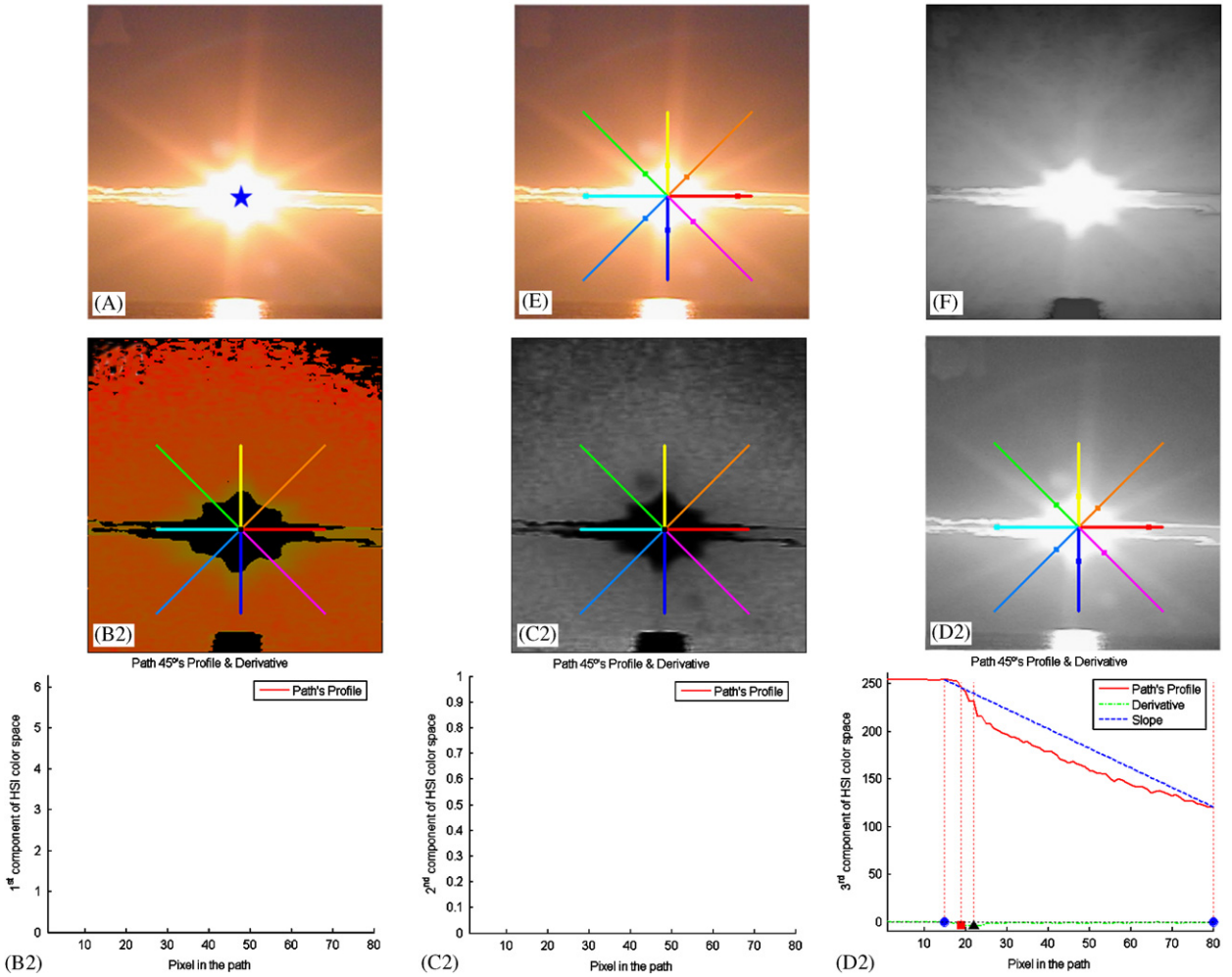


Fig. 7. Results obtained on a light shade with the proposed approach. A: the original image with the seed in the star. B1,C1,D1: the H, S, and I images, respectively, with paths used and the detected $\hat{v}$ points. B2,C2,D2: H, S, and I profiles for the 45° path, respectively. E: original image with the final first relevant color variation points detected in each direction. F: the final fuzzy region.

to adapt the function to the vertical asymptote, the slope must be raised to some power, as shown:

$$\lambda = \mathcal{F}(M) = \frac{1}{s \cdot |M|^t} - 1, \tag{13}$$

where $s$ is a scale factor and $t$ is a growth parameter. After a process of parameter estimation, we have obtained the best approximation to the function in Fig. 4, in the sense of minimum square error, for $s = 976$ and $t = 1.27$. The approximated function is in green color in Fig. 4. Though values in the vertical asymptote are not well approximated, the interesting values of $\lambda$ to model regions, the ones in $(-1, 1]$, have good approximations, with an error of $10^{-3}$ order.

## 5. Results

In this section, we present the results obtained by applying to real images the proposed approximation to automatically select $\lambda$. In all the experiments shown, we have chosen a set of eight paths covering eight homogeneously distributed directions from the seed: from 0° to 315°, with a step of 45°. Each path is the straight line formed by the sequence of

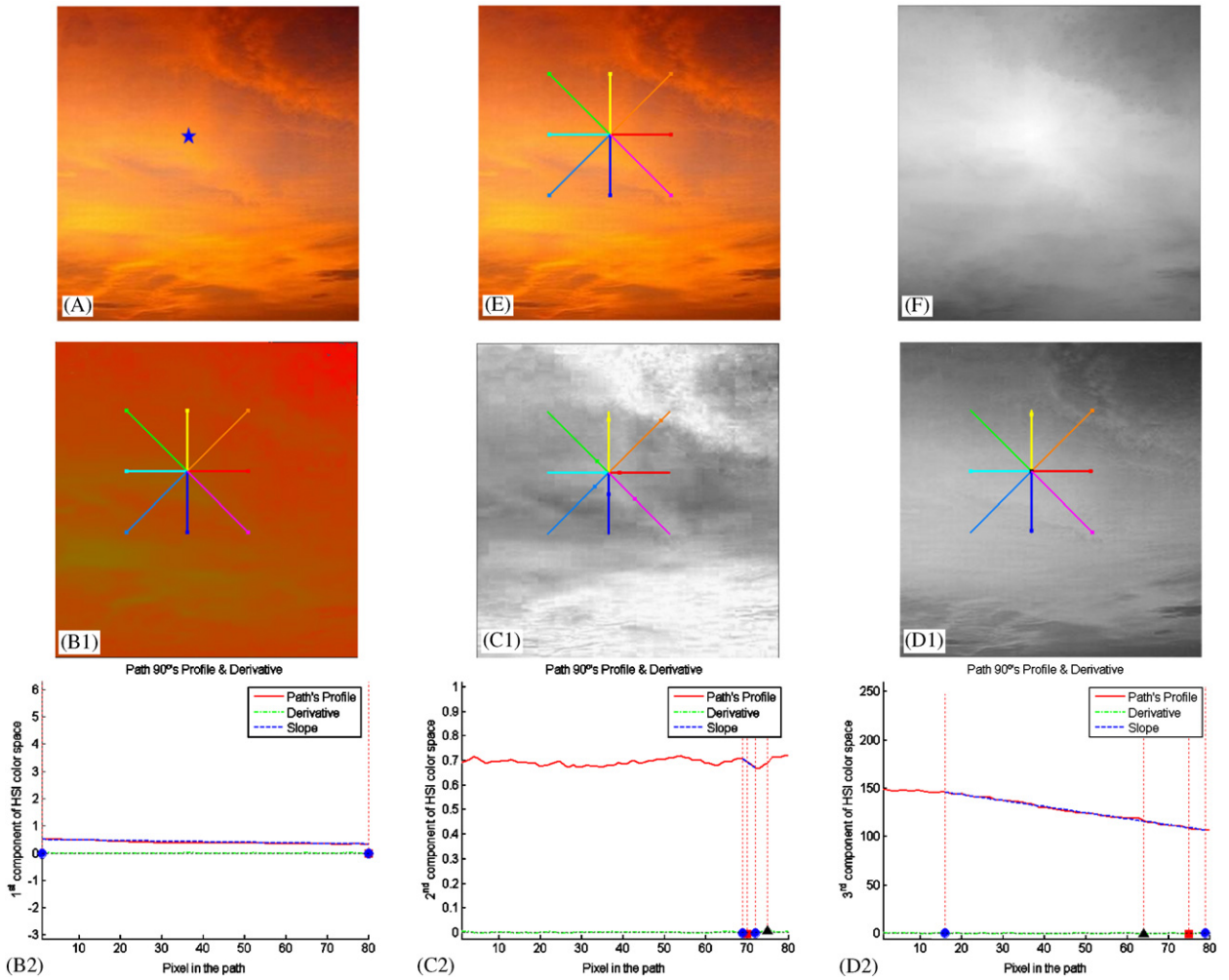


Fig. 8. Results obtained on an intensity tone down with small saturation changes, using the proposed approach. A: the original image with the seed in the star. B1,C1,D1: the H, S, and I images, respectively, with paths used and the detected $\hat{v}$ points. B2,C2,D2: H, S, and I profiles for the 90° path, respectively. E: original image with the final first relevant color variation points detected in each direction. F: the final fuzzy region.

consecutive pixels in the corresponding direction. The length of the paths has been fixed to 60, and the profile functions have been softened with a gaussian kernel of size 5 and $\sigma = 1$. The percentage used to compute the relevance threshold of a variation in each color channel is 75%.

Figs. 5–9 show the results obtained with the proposed automatization in different types of regions: a well defined region, a region with imprecise contours, a light shading, a tone down and a soft tone down, respectively. In all of those figures, the image A is the original image with a blue star at the seed point. Images (B1,C1,D1) of Figs. 5–9 represent the hue, saturation and intensity value of each pixel in the image, with the first relevant variation point found, in each path and color component, marked with a square. In addition, images (B2,C2,D2) of those figures show the hue, saturation and intensity profiles, respectively. These profiles correspond to the 0°, 180°, 45°, 90° and 0° paths in Figs. 5–9, respectively. Finally, image E represents the original image with the final location of the first relevant color variation point in each direction, and image F is the fuzzy model obtained with our approach for that region, using the $\lambda_s$ value indicated in the corresponding row of Table 1.

In Table 1 we numerically summarize these results. In the first column we identify the figure, and in the second column we show the $M_s$ obtained to characterize the magnitude of color variation in the contour of the area around the seed. The third column indicates the $\lambda_s$ value computed from this magnitude. As can be seen, when regions are

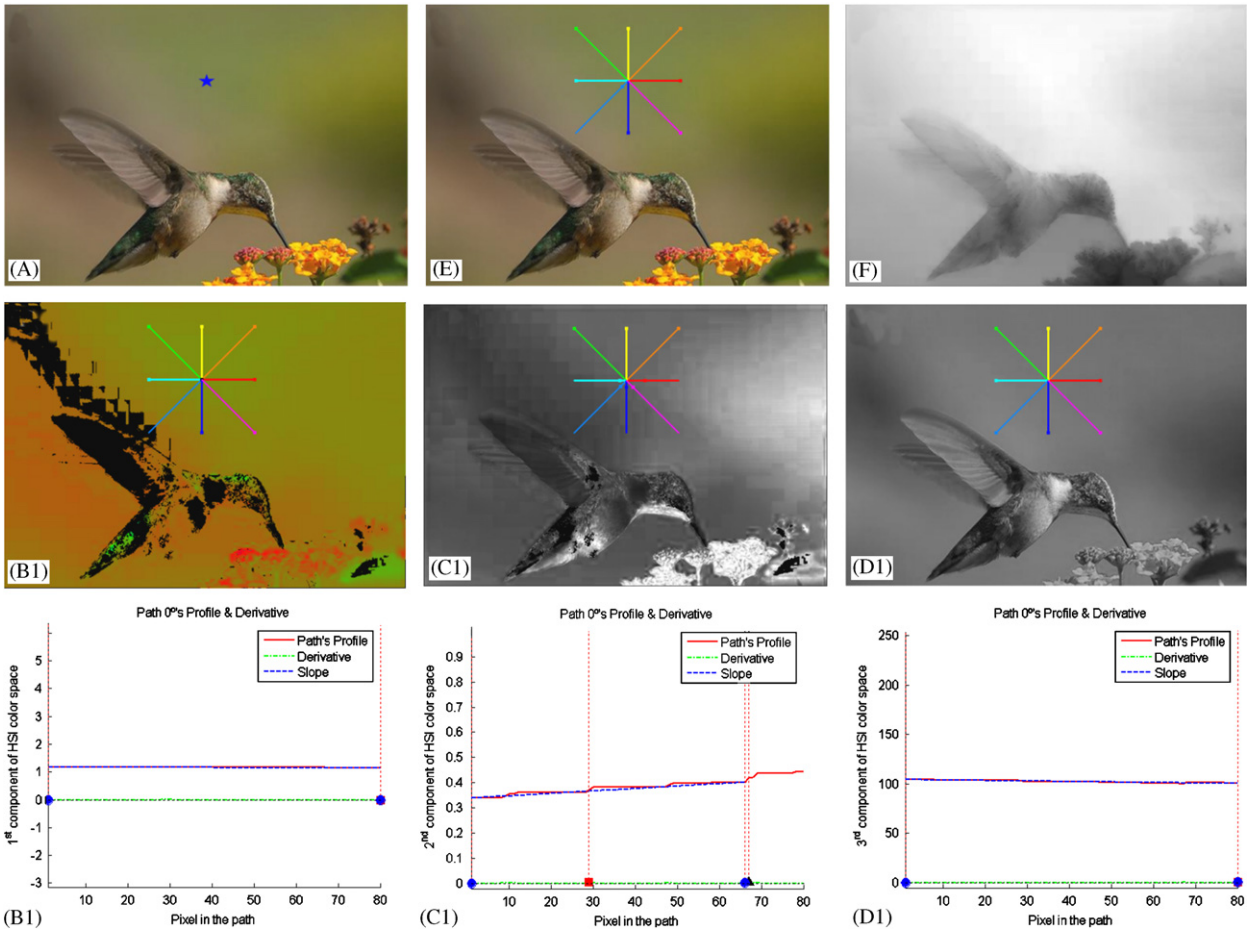


Fig. 9. Results obtained on soft saturation tone down with the proposed approach. A: the original image with the seed in the star. B1,C1,D1: the H, S, and I images, respectively, with paths used and the detected $\hat{v}$ points. B2,C2,D2: H, S, and I profiles for the 0° path, respectively. E: original image with the final first relevant color variation points detected in each direction. F: the final fuzzy region.

Table 1
$\lambda$ value obtained for each region

| Figure | $M_s$ | $\lambda$ |
|---|---|---|
| 5 | 0.046467 | −0.9495 |
| 6 | 0.011343 | −0.6973 |
| 7 | 0.003424 | 0.3860 |
| 8 | 0.000743 | 8.6437 |
| 9 | 0.000193 | 52.4603 |

homogeneous and with well defined contours, we obtain a "high" $M_s$ value, of $10^{-2}$ order, and a $\lambda_s$ value near to $-1$. As color variation in contours become softer, the $M_s$ value decreases, taking values of $10^{-3}$ order, and producing $\lambda_s$ values tending to 0. This value of $\lambda_s$ is reached and even exceeded when we have a soft tone down around the seed, whose $M_s$ value is of $10^{-4}$ order.

As can be seen in images (B1,C1,D1) of Figs. 5–7, the point detected in each path as the first relevant variation point coincides in most of the cases with the border of the region. On the other hand, in images (B1,C1,D1) of Figs. 8 and 9, we can see that in all the cases the square corresponding to the first relevant variation point is at the end of the path, indicating that there is no variation point, but that the whole path is a soft variation.

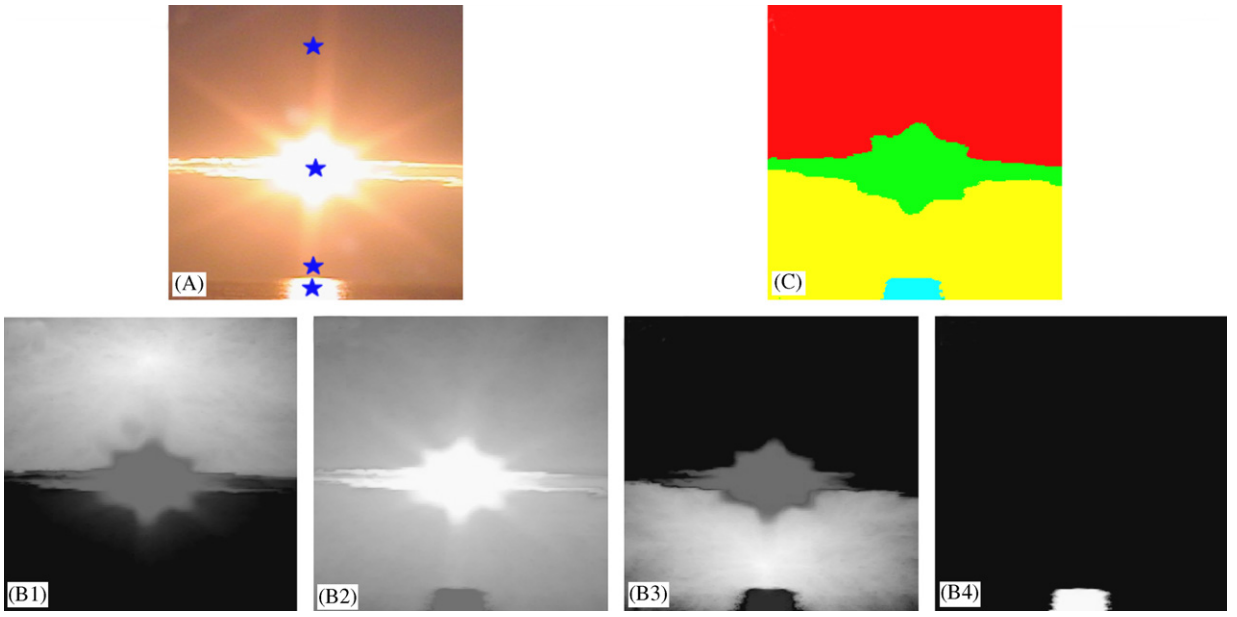


Fig. 10. Fuzzy segmentation. A: original image with seeds marked as blue stars. B1–B4: fuzzy regions corresponding to the seeds (from top to bottom). C: classification of pixels to the region that provides the maximum membership degree.

In these images we can also see how the slope of the line used in each profile to approximate the color variation magnitude (the dotted blue line) is higher in Figs. 5 and 6, where there is a big difference between the color inside the region and the one outside, than in Figs. 8 and 9, where we have a soft and gradual change of color.

In addition, we can compare the fuzzy models obtained for each kind of region, looking at the F images in Figs. 5–9, where a white gray level means maximum membership, while a black one corresponds to 0 membership degree. In the case of Fig. 5, corresponding to a well defined region with a significant color change at the borders, we can see that the membership value keeps constant and high inside the red area of the pepper, and decreases quickly as it reaches the borders.

Example of Fig. 6 corresponds to a region with imprecise contours where changes from the color inside the area around the seed to the one outside are gradual. It produces again constant and high around the seed, but gradually decreasing as the color changes. A similar behavior can be seen in the light bright in Fig. 7, where inside the homogeneous white sun membership degree is maximum, and softly decreases as the points grow apart from the light source.

The other extreme case is represented in Figs. 8 and 9 where profiles are plain or with a very small slope. Using the corresponding t-norm, we obtain a high membership degree in the whole fuzzy region, and a small decrease in the membership value at the borders. This makes the support of the region extented through almost the whole image, opposite to what happened in Fig. 5, where the support of the fuzzy region was only the area corresponding to the red pepper.

Finally, we show an example of the application of this technique in a segmentation problem in Fig. 10. Fig. 10(A) shows an image with four seeds placed corresponding to four regions, marked by blue stars. Figs. 10(B1–B4) show the fuzzy regions corresponding to those seeds (from top to bottom). In each case, we have obtained a suitable value of $\lambda$ as introduced in this paper. This is the final fuzzy segmentation of the image. If a crisp classification is needed, Fig. 10(C) shows the results of assigning each pixel to the region to which it pertains with higher degree.

## 6. Conclusions

We have presented a proposal to determine a suitable t-norm as aggregation functions to measure path homogeneity. The final objective is to use homogeneity measured this way in order to compute the membership function of fuzzy regions in fuzzy path-based color image segmentation.

We have chosen Weber's t-norm as reference since depending on its parameter value we obtain homogeneity measures with different behaviors, each of which fits a different type of region. Since regions we are interested in are homogeneously colored, differences between these types of regions are in their contours, so, given a seed, we approximate the color variation magnitude in the contour of the area surrounding it. Then, we use this magnitude representative of the kind of region to get, through a function approximated in this paper, the value of Weber's $\lambda$ parameter.

Results obtained with our approach show that this proposal provides suitable homogeneity measures, since the fuzzy regions obtained in each of the real image examples fit what we would intuitively expect. In addition, we have seen that, when regions are homogeneous with well defined contours, the magnitude of color variation at contours is of $10^{-2}$ order approximately, and the $\lambda$ value giving the homogeneity function is near to $-1$. Meanwhile, in tone down regions, this parameter is near 0 and even above it if the tone down is very soft, corresponding to magnitudes of color variation of $10^{-4}$ order. In the rest of the cases, these magnitudes are of order $10^{-3}$, and the value of $\lambda$ ranges between approximately $(-0.8, -0.3)$.

## References

[1] B.M. Cavalho, C.J. Gau, G.T. Herman, T.Y. Kong, Algorithms for fuzzy segmentation, Proc. Internat. Conf. on Advances in Pattern Recognition, 1999, pp. 154–163.
[2] J. Chamorro-Martinez, D. Sanchez, B. Prados-Suarez, A fuzzy color image segmentation applied to robot vision, in: J.M. Benitez, O. Cordon, F. Hoffman, R. Roy (Eds.), Advances in Soft Computing—Engineering, Design and Manufacturing, Springer, Berlin, 2003, pp. 129–138.
[3] J. Chamorro-Martinez, D. Sanchez, B. Prados-Suarez, E. Galan-Perales, M.A. Vila, A hierarchical approach to fuzzy segmentation of colour images, in: IEEE Internat. Conf. on Fuzzy Systems, vol. 2, St. Louis, Missouri (USA), May 2003, pp. 966–971.
[4] J. Chamorro-Martínez, D. Sánchez, B. Prados-Suarez, E. Galán-Perales, Fuzzy connectivity measures for path-based image segmentation, in: IEEE Internat. Conf. on Fuzzy Systems, Reno, Nevada (USA), May 2005, pp. 218–223.
[5] T.Q. Chen, Y. Lu, Color image segmentation—an innovative approach, Pattern Recognition 35 (2002) 395–405.
[6] H.D. Cheng, J. Li, Fuzzy homogeneity and scale-space approach to color image segmentation, Pattern Recognition 36 (7) (2003) 1545–1562.
[7] B.-C. Chien, M.-C. Cheng, A color image segmentation approach based on fuzzy similarity measure, in: Proc. 2002 IEEE Internat. Conf. on Fuzzy Systems, vol. 1, May 2002, pp. 449–454.
[8] R. Cucchiara, C. Grana, S. Seidenari, G. Pallancani, Exploiting color and topological gearures for region segmentations with recursive fuzzy c-means, Mach. Graphics and Vision 11 (2–3) (2002) 169–182.
[9] J. Delon, A. Desolneux, J.L. Lisani, A.B. Petro, Color image segmentation using acceptable histogram segmentation, in: Second Iberian Conf. on Pattern Recognition and Image Analysis, IbPRIA, 2005, pp. 239–246.
[10] P.M. Galaviz, A.R. Lopez, M.J.S. Garcia, I.H.P. Torres, Algorithm of clustering for color images segmentation, in: 15th IEEE Internat. Conf. on Electronics, Communications and Computers, 2005, pp. 306–310.
[11] F. Hacbouf, N. Mezhoud, An improved fuzzy rule-based segmentation system, in: Seventh Internat. Symp. on Signal Processing and Its Applications, July 1–4, 2003, vol. 1, 2003, pp. 533–536.
[12] J. Han, K.-K. Ma, Fuzzy color histogram and its use in color image retrieval, IEEE Trans. Image Process. 11 (8) (2002) 944–952.
[13] G.T. Herman, B.M. Carvalho, Multiseeded segmentation using fuzzy connectedness, IEEE Trans. Pattern Anal. Mach. Intell. 23 (5) (2001) 460–474.
[14] M. Kazanov, A new color image segmentation algorithm based on watershed transformation, in: 15th IEEE Internat. Conf. on Electronics, Communications and Computers, 2004, pp. 590–593.
[15] O. Lezoray, An unsupervised color image segmentation based on morphological 2d clustering and fusion, in: VI Internat. Symp. on Multispectral Color Science, vol. 2004: 173-7, 2004, pp. 173–177.
[16] J. Maeda, X. Dai, Y. Suzuki, Unsupervised segmentation of textured color images using fuzzy homogeneity decision, in: 4th EURASIP-IEEE Region 8 Internat. Symp. on Video/Image Processing and Multimedia Communications, vol. 1, June 2002, pp. 75–78.
[17] J. Maeda, C. Ishikawa, S. Novianto, N. Tadehara, Y. Suzuki, Rough and accurate segmentation of natural color images using fuzzy region-growing algorithm, in: 15th Internat. Conf. on Pattern Recognition, vol. 3, October 2000, pp. 638–641.
[18] J. Maeda, S. Saga, Y. Suzuki, Rough segmentation of natural color images using fuzzy-based hierarchical algorithm, in: The 2004 47th Midwest Symp. on Circuits and Systems, vol. 1, July 2004, pp. 217–220.
[19] S. Makrogiannis, G. Economou, S. Fotopoulos, N.G. Bourbakis, Segmentation of color images using multiscale clustering and graph theoretic region synthesis, IEEE Trans. Systems Man and Cybernetics, Part A, Systems and Humans 35 (2) (2005) 224–238.
[20] N. Mezhoud, I. Merzoug, R. Boumaza, M.C. Batouche, Color image segmentation using a new fuzzy clustering method, in: IEEE Internat. Conf. on Industrial Technology, vol. 3, 2004, pp. 1209–1214.
[21] A. Moghaddamzadeh, N. Bourbakis, A fuzzy region growing approach for segmentation of color images, Pattern Recognition 30 (6) (1997) 867–881.
[22] E. Navon, O. Miller, A. Averbuch, Color image segmentation based on adaptive local thresholds, Image and Vision Comput. 23 (1) (2005) 69–85.
[23] S. Romani, P. Sobrevilla, E. Montseny, On the reliability degree of hue and saturation values of a pixel for color image classification, in: IEEE Internat. Conf. on Fuzzy Systems 2005, 2005, pp. 306–311.
[24] A. Rosenfeld, Fuzzy digital topology, Inform. and Control 40 (1) (1979) 76–87.

[25] J. Udupa, S. Samarasekera, Fuzzy connectedness and object definition: theory, algorithms and applications in image segmentation, Graphical Models and Image Proc. 58 (3) (1996) 246–261.
[26] C. Wanhyun, J. Park, M. Lee, S. Park, Unsupervised color image segmentation using mean shift and deterministic annealing EM. in: Internat. Conf. on Computational Science and Its Applications, ICCSA, vol. 3, 2004, pp. 867–876.
[27] Y. Zhao, M. Li, A modified fuzzy c-means algorithm for segmentation of MRI, Proc. Fifth Internat. Conf. on Computational Intelligence and Multimedia Applications (ICCIMA 2003), 27–30 September, 2003, pp. 391–395.